Journal of Power Sources 202 (2012) 332–335

Contents lists available at SciVerse ScienceDirect

Journal of Power Sources

journal homepage: www.elsevier.com/locate/jpowsour

Short communication

Electrochemical performance of an all-solid-state lithium ion battery with garnet-type oxide electrolyte

Shingo Ohta*, Tetsuro Kobayashi, Juntaro Seki, Takahiko Asaoka

Toyota Central R&D Labs. Inc., 41-1 Yokomichi, Nagakute, Aichi 480-1192, Japan

ARTICLE INFO

Article history:
Received 6 June 2011
Received in revised form 29 August 2011
Accepted 17 October 2011
Available online 20 October 2011

Keywords:
All-solid-state lithium ion battery
Solid electrolyte
Oxide ceramics
Electrochemical property

ABSTRACT

The electrochemical performance and charge transfer resistance of an all-solid-state lithium ion battery consisting of $LiCoO_2$ (LCO; cathode), $Li_{6.75}La_3Zr_{1.75}Nb_{0.25}O_{12}$ (LLZONb; solid electrolyte), and lithium (anode) were investigated. This battery has favorable charge–discharge behavior and exhibits good stable cycle performance. No other reaction phase or exfoliation was evident at the interface between LCO and LLZONb after 100 charge–discharge cycles. The interfacial resistance between LCO and LLZONb is comparable to that of lithium ion batteries with liquid organic electrolytes, and the activation energy of the interfacial resistance of this battery is still lower than that of a lithium ion battery with a liquid organic electrolyte.

1. Introduction

All-solid-state lithium ion batteries that employ a solid electrolyte are generally considered to be safer than those that use liquid organic electrolytes by removing the issue of flammability. In order to improve the performance of all-solid-state lithium ion batteries, an appropriate solid oxide electrolyte is strongly required that has the following properties: (1) high lithium ion conductivity, (2) stability against chemical reaction with lithium at the anode, and Co-, Ni-, or Mn-containing oxides at the cathode, and (3) a wide electrochemical window allowing the use of high-voltage cathode materials.

Solid oxides electrolytes are believed to have a potential advantage over other inorganic materials in terms of their handling and chemical stability. However, most solid oxide electrolytes have lower lithium ion conductivity than other electrolytes, such as commonly utilized liquid organic electrolytes or solid sulfide electrolytes [1–4].

We have focused on the garnet-type oxide $Li_7La_3Zr_2O_{12}$ (LLZO) [5] as a promising candidate for solid oxide electrolytes, due to its high chemical stability and wide potential window. However, the lithium ion conductivity of LLZO is ca. 0.2 mS cm^{-1} at 25 °C, which is approximately two orders of magnitude lower than that of common liquid organic electrolytes. Very recently, we have optimized the composition of LLZO by substitutional Nb-doping to improve the lithium ion conductivity, and a maximum of ca. 0.8 mS cm^{-1} at 25 °C was obtained by doping Nb at 12.5 at% [6].

Application of lithium ion batteries such as in electric vehicles (EV) and hybrid electric vehicles (HEV) requires high-power, high-capacity, and long battery life. To improve these characteristics of lithium ion batteries, it is very important to decrease the internal resistance. Generally, the dominant contributor to the internal resistance of all-solid-state lithium ion batteries is not the bulk resistance of the solid electrolyte, but the interfacial resistance between the electrodes and solid electrolyte [1–4]. Very recently, electrochemical performance of all-solid-state lithium ion battery using LLZO, which was constructed by sol-gel method, has been reported [7]. However, the interfacial resistance is still large because the charge transfer resistance would be strongly affected by interfacial contact condition. The interfacial contact condition between LLZO bulk ceramics and LCO prepared by sol–gel method would not be likely enough. Therefore, the intrinsic electrochemical performance and interfacial resistance of all-solid-state lithium ion battery using LLZO is still unknown. In order to clarify the electrochemical performance and interfacial resistance of between cathode and Nb-doped LLZO, an all-solid-state lithium ion battery was fabricated using Nb-doped LLZO (LLZONb; solid electrolyte), lithium (anode), and $LiCoO_2$ (LCO; cathode), which was deposited by pulsed-laser deposition (PLD). Here we report the electrochemical performance and interfacial resistance of this battery.

2. Experiment

An all-solid-state lithium ion battery was constructed using LLZONb, Li, and LCO. LLZONb ($Li_{6.75}La_3Zr_{1.75}Nb_{0.25}O_{12}$) was

* Corresponding author. Tel.: +81 561 71 7659; fax: +81 561 71 5743.
E-mail address: sohta@mosk.tytlabs.co.jp (S. Ohta).

0378-7753/$ – see front matter © 2011 Elsevier B.V. All rights reserved.
doi:10.1016/j.jpowsour.2011.10.064

fabricated by conventional solid-state reaction [6], and a 2 mm thick, 13 mm diameter bulk LLZONb pellet was prepared. LCO was deposited by PLD (4ω-Nd:yttrium–aluminum–garnet (YAG) laser, $\lambda = 266$ nm, ~1 J cm^{-2} pulse^{-1}, ~20 ns, 10 Hz) on the top side of the sintered LLZONb pellet and annealing at 600 °C. The deposited thickness of the LCO film was ca. 500 nm, which was estimated from cross-sectional field emission scanning electron microscopy (FE-SEM/Hitachi S-5500) image. The lithium metal foil anode was attached to the bottom of the pellet in a dry Ar-filled glove box. The morphology and elementary analysis of the interface of this battery was observed using FE-SEM and Energy dispersive X-ray analysis EDX (Horiba EMAX energy EX-350). The electrochemical properties, such as the charge and discharge characteristics were evaluated under galvanostatic condition of 3.5 μA cm^{-2} (rate: 0.1 C) in the 4.2–2.5 V range at 25 °C using a potentio-galvanostat (Solartron 1480). The interfacial resistance of the battery was measured using an impedance analyzer (Solartron FRA 1255B) in the frequency range of 0.1 Hz to 1 MHz.

3. Result and discussion

Fig. 1 shows charge–discharge curves of the all-solid-state lithium ion battery. The plateau of the charge curve starts at approximately 3.7 V, which is slightly lower than the conventional extraction/insertion reaction of LCO (3.9 V), due to the lower crystallinity of LCO [8,9] prepared by PLD. The theoretical electrochemical capacity of LCO is 137 mAh g^{-1}, which corresponds to 0.5 Li per CoO_2. The charge and discharge capacity at the 1st cycle were 130 and 129 mAh g^{-1}, respectively, which are approximately 90% of the theoretical capacity. The charge–discharge curves at the 100th cycle are shown by the dotted line in Fig. 1. The charge and discharge capacity at the 100th cycle were 130 and 127 mAh g^{-1}, respectively. The retention of discharge capacity was approximately 98%, which confirms stable cycle performance for this battery.

Fig. 2 shows a cross-sectional FE-SEM image and EDX mapping of the interface between LCO and LLZONb after 100 charge–discharge cycles. No other reaction phase or exfoliation are evident at the interface. Elementary analysis due to EDX confirmed that no elemental diffusion occurred near the interface. Although Dr. Kim et al. reported that reaction phases due to mutual diffusion are easily formed between LLZO and LCO at the interface [10]. They suggested that the reaction layer formed during high temperature processing is likely one of the major reasons for the poor lithium insertion/extraction at LLZO/LCO interfaces. We considered that cause of this difference would be the following reasons. (1) The annealing temperature of LCO was different. (2) Difference of composition for garnet-type oxide. Therefore, the all-solid-state lithium ion battery constructed in this study would have chemical and structural stability during lithium intercalation/deintercalation through the charge and discharge processes.

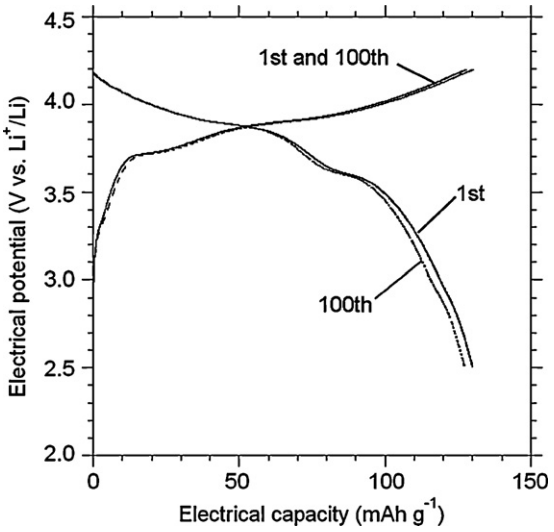

Fig. 1. Charge–discharge curves for the $LiCoO_2/Li_{6.75}La_3Zr_{1.75}Nb_{0.25}O_{12}$/Licell. The horizontal axis shows the capacity normalized by the weight of the $LiCoO_2$ cathode. Solid and dotted lines represent the 1st and 100th charge–discharge cycles, respectively.

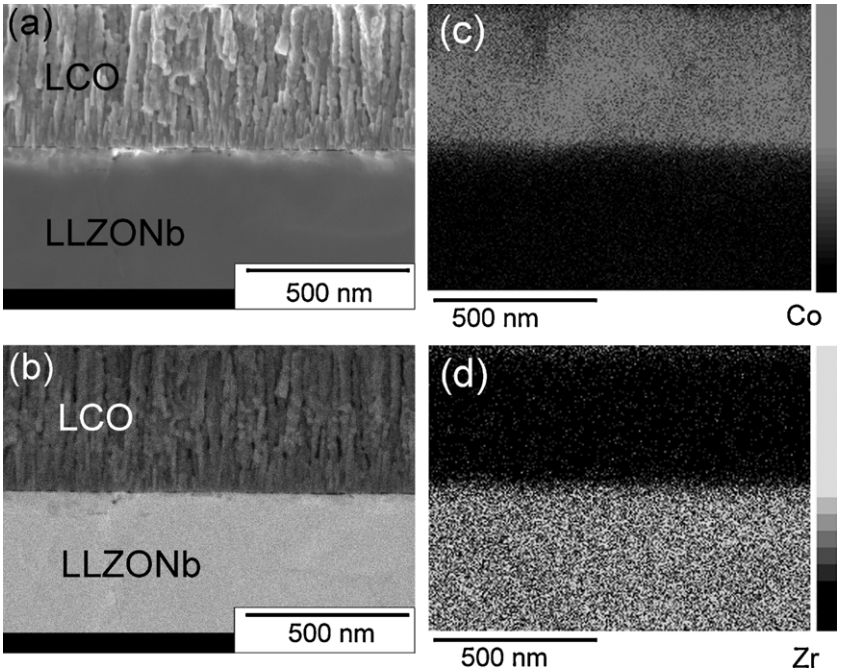

Fig. 2. Cross-sectional FE-SEM secondary electron (a) and backscattering electron (b) image of the interface between $LiCoO_2$ and $Li_{6.75}La_3Zr_{1.75}Nb_{0.25}O_{12}$ after 100 charge–discharge cycles. EDX mapping for Co (c) and Zr (d).

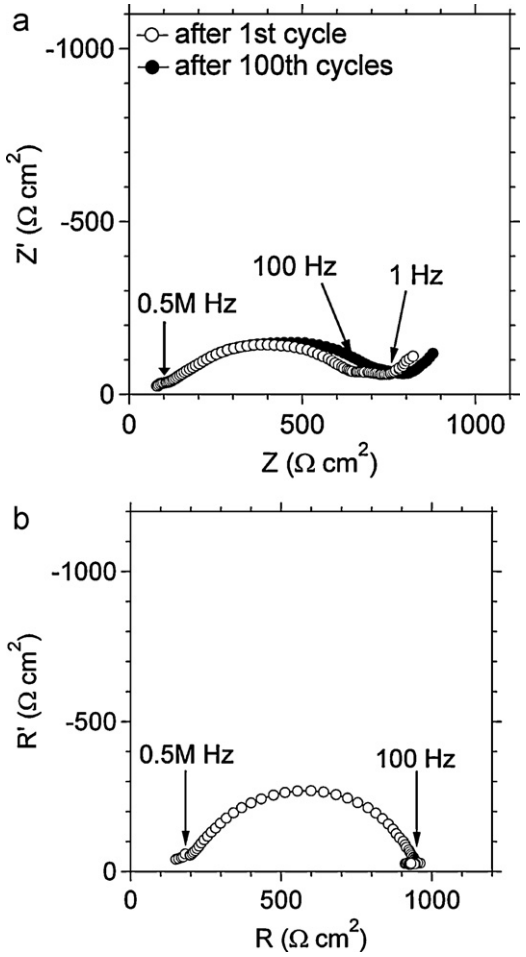

Fig. 3. (a) Nyquist plot (0.1 Hz to 1 MHz) for the $LiCoO_2/Li_{6.75}La_3Zr_{1.75}Nb_{0.25}O_{12}/Li$ cell at 3.95 V. (b) Nyquist plot (0.1 Hz to 1 MHz) for the $Li/Li_{6.75}La_3Zr_{1.75}Nb_{0.25}O_{12}/Li$ cell.

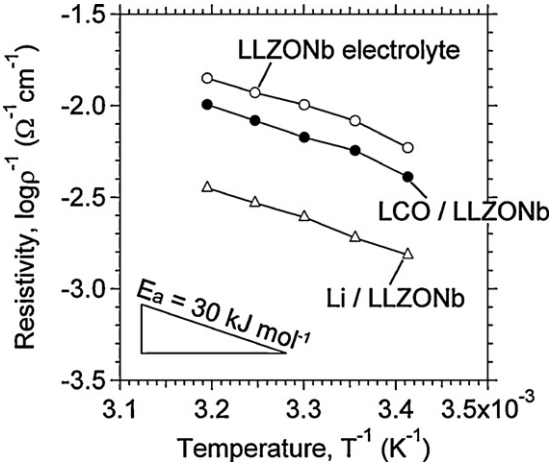

Fig. 4. Temperature dependence of the resistivity (ρ) for $Li_{6.75}La_3Zr_{1.75}Nb_{0.25}O_{12}$ bulk, the $LiCoO_2/Li_{6.75}La_3Zr_{1.75}Nb_{0.25}O_{12}$ interface and the $Li/Li_{6.75}La_3Zr_{1.75}Nb_{0.25}O_{12}$ interface.

The interfacial resistance of the battery was evaluated using a two-probe AC impedance method. Measurements were conducted after charging at 3.95 V vs. Li^+/Li. A Nyquist plot for the all-solid-state lithium ion battery is shown by the open circles in Fig. 3(a). Three resistance components are evident, with frequencies at approximately 0.5 MHz, 100 Hz, and 1 Hz, which can be well-resolved into resistance of the LLZONb bulk (R_{LLZONb}) [6], the interface between LCO and LLZONb ($R_{LCO/LLZONb}$), and the interface between Li and LLZONb ($R_{Li/LLZONb}$), respectively. To identify the frequency dependence of the interfacial resistance between Li and LLZONb, we constructed a Li/LLZONb/Li cell with lithium metal foils attached to both LLZONb faces. The Nyquist plot for this cell is presented in Fig. 3(b), which indicates that $R_{Li/LLZONb}$ is approximately 100 Hz. Therefore, the resistance component at approximately 1 Hz is assigned to $R_{LCO/LLZONb}$. The resistivity at 3.95 V vs. Li^+/Li was calculated from Fig. 3(a) and the resistivities for R_{LLZONb}, $R_{LCO/LLZONb}$ and $R_{Li/LLZONb}$ were 120, 170 and 530 Ω cm^2, respectively. A Nyquist plot for the all-solid-state lithium ion battery after 100 charge–discharge cycles is shown by the solid circles in Fig. 3(a). The interfacial resistance has not almost changed during 100 charge–discharge cycles. Therefore it is considered that interface between LCO and LLZONb has a good stable cycle performance.

$R_{LCO/LLZONb}$ is low compared to the resistances of other interfaces between cathodes and other electrolytes such as sulfide materials or liquid organic electrolytes [2,4]. Takada and his group investigated all-solid-state lithium ion batteries with solid sulfide electrolytes and suggested that large space-charge layers are grown between the oxide electrode and sulfide electrolyte because Li ion transfer from the sulfide electrolyte to the oxide electrode occurs by the large difference in chemical potential [2]. Therefore, the interfacial resistance between the oxide electrode and sulfide electrolyte is large (ca. 1000 Ω). In order to overcome this problem, they coated LCO with an oxide electrolyte such as $LiNbO_3$ or $Li_4Ti_5O_{12}$ and successfully decreased the interfacial resistance between the cathode and electrolyte [2,3]. In contrast, it is considered that space-charge layers grown on the interface between LCO and LLZONb would be small because the difference in chemical potential between LCO and LLZONb should be smaller than that between LCO and a sulfide electrolyte; therefore, $R_{LCO/LLZONb}$ is rather low.

The temperature dependence of R_{LLZONb}, $R_{LCO/LLZONb}$ and $R_{Li/LLZONb}$ are shown in Fig. 4. The activation energy (E_a) of the interfacial resistance was calculated from the Arrhenius law ($\rho^{-1} = A\exp(-E_a/kT)$, where A is the frequency factor, k is the Boltzmann constant, and T is the absolute temperature). E_a for both $R_{LCO/LLZONb}$ and $R_{Li/LLZONb}$ were ca. 30 kJ mol^{-1}, which are much lower than that for the interface between LCO and liquid organic electrolytes (ca. 60 kJ mol^{-1}) [11]. The reason for this phenomenon can be understood as follows. It is considered that desolvation reaction occurs with lithium ion transfer at the interface between the electrodes and a liquid organic electrolyte. Therefore, E_a of the interfacial resistance between electrodes and liquid organic electrolytes are quite large (ca. 60 kJ mol^{-1}) [12–17]. However, in an all-solid-state lithium ion battery, the desolvation reaction does not occur; therefore, E_a of both $R_{LCO/LLZONb}$ and $R_{Li/LLZONb}$ would be expected to be the same as that for the LLZONb bulk electrolyte.

4. Conclusions

An all-solid-state lithium ion battery of LCO/LLZONb/Li was constructed. The charge and discharge capacity of this battery at the 1st cycle were 130 and 129 mAh g^{-1}, respectively, which is approximately 90% of the theoretical capacity. This battery exhibited stable cycle performance, with no other reaction phase or exfoliation at the interface after 100 charge–discharge cycles. The interfacial resistance between LCO and LLZONb at 25 °C was 170 Ω cm^2, which is comparable to that for a lithium ion battery with a liquid organic electrolyte. The activation energy of interfacial resistance between LCO and LLZONb was lower than that for a lithium ion battery with a liquid organic electrolyte. These results indicate that LLZONb is a promising candidate as a solid electrolyte for high-power and high-capacity all-solid-state lithium ion batteries.

References

[1] K. Takada, T. Inada, A. Kajiyama, H. Sasaki, S. Kondo, M. Watanabe, M. Murayama, R. Kanno, Solid State Ionics 158 (2003) 269.
[2] N. Ohta, K. Takada, L.-Q. Zhang, R.-Z. Ma, M. Osada, T. Sasaki, Adv. Mater. 18 (2006) 2226.
[3] N. Ohta, K. Takada, I. Sakaguchi, L. Zhang, R. Ma, K. Fukuda, M. Osada, T. Sasaki, Electrochem. Commun. 9 (2007) 1486.
[4] A. Sakuda, H. Kitaura, A. Hayashi, K. Tadanaga, M. Tatsumisago, Electrochem. Solid State Lett. 11 (2008) A1.
[5] R. Murugan, V. Thangadurai, W. Weppner, Angew. Chem. Int. Ed. 46 (2007) 7778.
[6] S. Ohta, T. Kobayashi, T. Asaoka, J. Power Sources 196 (2011) 3342.
[7] M. Kotobuki, H. Munakata, K. Kanamura, Y. Sato, T. Yoshida, J. Electrochem. Soc. 157 (2010) A1076.
[8] W. Huang, R. Frech, Solid State Ionics 86–88 (1996) 395–400.
[9] R.J. Gummow, M.M. Thackeray, Mater. Res. Bull. 27 (1992) 327–337.
[10] K.-H. Kim, Y. Iriyama, K. Yamamoto, S. Kumazaki, T. Asaka, K. Tanabe, C.A.J. Fisher, T. Hirayama, R. Murugan, Z. Ogumi, J. Power Sources 196 (2011) 764.
[11] Y. Iriyama, T. Kako, C. Yada, T. Abe, Z. Ogumi, Solid State Ionics 176 (2005) 2371.
[12] I. Yamada, T. Abe, Y. Iriyama, Z. Ogumi, Electrochem. Commun. 5 (2003) 502.
[13] Z. Ogumi, T. Abe, T. Fukutsuka, S. Yamate, Y. Iriyama, J. Power Sources 127 (2004) 72.
[14] T. Abe, H. Fukuda, Y. Iriyama, Z. Ogumi, J. Electrochem. Soc. 151 (2004) A1120.
[15] S. Kobayashi, Y. Uchimoto, J. Phys. Chem. 109 (2005) 13322.
[16] T. Abe, F. Sagane, M. Ohtsuka, Y. Iriyama, Z. Ogumi, J. Electrochem. Soc. 152 (2005) A2152.
[17] F. Sagane, T. Abe, Z. Ogumi, J. Power Sources 195 (2010) 7466.